Computer simulation of real-world vehicle–pedestrian impacts

Ramamurthy, P. , Blundell, M.V. , Bastien, C. and Zhang, Y.

Computer Simulation of Real-World Vehicle-Pedestrian Impacts

P. Ramamurthy, M. Blundell, C. Bastien, Y. Zhang

Faculty of Engineering and Computing, Coventry University, Coventry, CV1 5FB, UK

Pradeep Ramamurthy - magadirp@coventry.ac.uk , pradeep0891@yahoo.com
Michael Victor Blundell - cex403@coventry.ac.uk
Christophe Bastien - aa3425@coventry.ac.uk
Yingshun Zhang – yingshun.zhang@gmail.com

Computer Simulation of Real-World Vehicle-Pedestrian Impacts

P. Ramamurthy[*], M. Blundell[†], C. Bastien[‡], Y. Zhang

Faculty of Engineering and Computing, Coventry University, Coventry, CV1 5FB, UK

Abstract:

This paper describes a study carried out to develop and apply computer analysis tools to simulate real world accidents between vehicles and pedestrians. The main focus has been the incorporation of realistic pedestrian pre-impact gait motion and to investigate the outcome of real world impacts. A combination of Multi-Body (MB), FACET and Finite Element (FE) based vehicle models in conjunction with validated human body models developed by MADYMO were used to simulate and analyse vehicle-pedestrian accident scenarios.
European regulations and consumer tests for passenger cars now address vehicle front aggressiveness, and vehicle manufactures have effectively developed design solutions meeting these requirements. Vehicle frontal geometry and pedestrian pre-impact characteristics play a major role in determining the post-impact kinematics and severity of injury sustained during pedestrian- vehicle contact stage.
A unique aspect of this study has been the application of the Injury Severity Index (IrSiX) method developed for automotive occupant injury assessment to pedestrians. The injury results from the simulations were measured and the severity assessed applying a quantitative rating method.

Keywords: Pedestrian, Accident Simulation, Pedestrian Safety, Vehicle-Pedestrian Impact.

1. Introduction

As we move further into the new millennium, following over 100 years of motor vehicle production, the automotive industry has made continuous progress in the development of safety devices that provide drivers and passengers with high levels of protection during a vehicle crash. Until recently the safety of pedestrians and other vulnerable road users from a vehicle design point of view has received little attention. The growth of the economy has given rise to the increase in motor vehicles and volume of road traffic. In Great Britain, there was a 78 percent increase in registered

[*] Author. Email: pradeep0891@yahoo.com
[†] Corresponding author. Email: cex403@coventry.ac.uk
[‡] Corresponding author. Email: aa3425@coventry.ac.uk

road vehicles between 1980 and 2008, from 19.2 to 34.2 million [1]. Increasing motorization has created a demand for more road space, and the lack of which has resulted in large numbers of fatalities to vulnerable road users such as pedestrians and cyclists.

According to the Transport Statistics Bulletin [2], 7,188 pedestrians were killed or seriously injured in the UK alone and approximately 40,000 fatalities occur in Europe each year. The automotive industry is turning its attention to the exterior of the vehicle and the design of "pedestrian friendly" vehicles in order to respond to proposed developments in legislation such as the EEVC WG17 [3] test procedures.

In this study, work has been carried out to extend the simulations beyond the test procedures and simulate using MADYMO [4] pedestrian impact events as realistically as possible. The emphasis has been on the application of real-world vehicle dynamics and initial pedestrian motion to examine primary impacts and post impact kinematics of the pedestrian. A simulation matrix was designed to recreate pedestrian to vehicle impacts across a wide range of vehicle dynamics, pedestrian kinematics and impact configurations. Four different vehicle types have been considered. The results were analyzed by adopting the IrSiX methodology to represent critical parameters relating to the pedestrian impacts and to generate statistical models for various responses such as pedestrian throw distance, femur shear force and knee bending angle.

2. Methodology

The work to date by the majority of researchers in the field of pedestrian impact analysis, has involved analysing models where the pedestrian is stationary, in a set posture. The study carried out by Kühnel [5] stated that static dummy tests do not

provide sufficient information to reconstruct real world pedestrian accidents. Further investigation of real world accident cases [5, 6, 7] suggests that the pedestrian initial movement can considerably influence the dynamic behaviour of the collision and post impact kinematics of the pedestrian.

Video evidence and results from field studies of pedestrian crossings [8, 9, 10, 11] show that pedestrians are more likely to be walking or running when they cross into the path of an oncoming vehicle and suffer an impact. Stammen [12] investigated 521 pedestrian accident cases of which 51% of pedestrians were walking, 28% were reported to be running or jogging. No more than 10% of the pedestrians were standing still in the path of an oncoming vehicle and the rest of the pedestrians' movements (10%) were inconclusive.

Studies carried out by LeGlatin [13] and Meissner [14] demonstrate that the resulting post impact kinematics of the pedestrian is sensitive to pre-impact motion and posture. In his work LeGlatin modelled pedestrian motion by applying an overall initial velocity to the pedestrian without progressing to the incorporation of gait motion. As such the initial velocity of the pedestrian dummy does not model a walking or running pedestrian but rather a pedestrian sliding in a direction transverse to the oncoming vehicle.

In this study, in order to incorporate real world pedestrian pre-impact motion for the MADYMO pedestrian model, human gait motion was analyzed using the VICON MX optical motion capture system, at Coventry University. Walking and running gait data were recorded from instrumented tests on volunteers. Using the VICON gait report, values of joint angles of the hip, knee, and ankle were derived and joint motion as a function of time was prescribed to the pedestrian model to achieve walking and running motion.

According to statistics [15] the casualty rates are slightly greater for males than females and numerically the most at risk group are males in the age range 25-59 years. Hence a MADYMO 50th percentile male pedestrian model was used to simulate the vehicle-pedestrian interaction [31].

A range of vehicle models (Figure 1) was used for this study to represent the following vehicle types, a small segment vehicle based on a 1994 model Vauxhall Corsa, a medium segment vehicle based on Chrysler Neon, a people carrier van based on a Chrysler voyager and a Sports Utility Vehicle (SUV) model based on the Ford Explorer. These vehicle models are based on public domain models used by the NHTSA with the aim to recreate realistic vehicle-pedestrian accident simulations. The vehicle models were re-configured to be used in the MADYMO solver environment, applying refinement techniques to minimise the overall computational time.

The front end geometry of the vehicle models is made up of interconnected FE sub-models (Figure 2), in contrast to the body shell of the vehicle, which is modelled using rigid FACET bodies. The material and stiffness characteristics for the front end of the vehicles have been derived from LeGlatin [16]. The realism of the models was established by performing simulated EEVC WG10 impactor tests on the front end of the vehicles using validated MADYMO impactor models [17, 18]. The tests conducted were: the headform impactor to bonnet top test [32], the legform impactor [33] to bumper test and the upper legform impactor to bonnet leading edge test [34]. Analysis of the results indicated that the MADYMO FE/FACET vehicle models and the pedestrian sub-system tests have rightly predicted the kinematics and injury severity showing good agreement when compared with physical test results.

Consequently it was established that the FE/FACET vehicle models developed during this stage could be further used for recreating detailed vehicle-pedestrian accident simulations with confidence.

3. Vehicle Model Validation and Simulation of Pedestrian Pre-Impact Motion

3.1 Validation of Vehicle Models

The use of multi-body techniques for the representation of the vehicle-pedestrian impact (Figure 2) has proven successful for the simulation of body segment displacement and also visual comparison of the pedestrian model kinematics when compared to trajectories of cadaver tests conducted by Ishikawa [19]. multi-body techniques are reliable when predicting pedestrian kinematics but have limitations to predict injury severity. By using the FE vehicle models, more representative results can be obtained which can then be related to injury severity.

Responses of the pedestrian model were reproduced for a set of cadaver test configurations. Tests were simulated at impact speeds of 32km/h and 40km/h. The simulation evaluates the vehicle characteristics such as stiffness and structural response. The pedestrian was positioned in a walking posture, with the leg projected forward and balanced similarly to the test carried out by Ishikawa [20]. The post-impact trajectories of the pedestrian, namely the head, pelvis, knee and the ankle were extracted from the simulation results for comparative analysis with the published cadaver test trajectories. Figures 3, 4, 5 and 6 provide examples of the results extracted from the correlation study.

The results from the pedestrian full body trajectory analysis simulated at 32km/h with a mid-size car are shown in Figure 3. These results have been compared with Ishikawa's post-mortem human subjects (PMHS) test (solid trend line)[21] and LeGlatin's FE model tests (dotted trend line)[16]. Overall, the trajectory results

demonstrate a satisfactory correlation with published PMHS test data. Due to the differences in the geometry of the vehicle used, minor differences were observed.

From Figure 4 the head velocity response can be analysed. The resultant head velocity time history shows similar behaviour but does not correlate well when compared with the cadaver test due to the characteristic differences in vehicle geometries.

FE and multi-body vehicle models were used to analyze a pedestrian accident scenario at 32km/h impact velocity, the resulting head and tibia acceleration curves were compared to the PMHS test results [21,22] (Figures 5 and 6). A time offset on the peak acceleration can be observed (Figure 5) between simulations. The FE model head accelerations tend to peak later than the acceleration peak of the MBS vehicle model. This is due to the minor structural differences at the contact area between the two models. In Figures 5 and 6, the acceleration curves derived from mid-size vehicle models are compared with acceleration curves derived from PMHS impacts. A difference of 11% is observed in the peak acceleration value between the two impacts. Considering the fact that the mathematical model to have minor differences in material and geometrical characteristics when compared with the PMHS test and as far as the behaviour of the acceleration curve is concerned, the outcome is within a reasonable agreement.

The tibia accelerations in Figure 6 were compared to the results derived from the PMHS test conducted by Masson and Serre [22]. The accelerations are derived during the first 25ms because the PMHS study has been focused on knee and leg injuries associated with the front bumper impact. The FE vehicle models show better result correlation when compared with results derived from simulations with MB vehicle model.

Following the validation of the FE vehicle model at 32km/h, similar tests were conducted at a higher impact speed of 40km/h. The output results were compared to Ishikawa's PMHS tests conducted at 40km/h. A good correlation was observed between the PMHS and FE vehicle model test results. Consequently it was concluded that the FE vehicle models coupled with the MADYMO pedestrian models were sensitive enough to carry out a parametric study.

3.2 Pedestrian Pre-Impact Motion

Analysing the GIDAS (German In-Depth Accident Study) documented by the Accident Research Unit at Medical University Hannover [23], a majority of pedestrians were found to be walking or running prior to a vehicle collision. Phases that are involved in human walking and running gait were examined by conducting gait analysis using the VICON motion capture system (Figure 7) and also the mechanics of weight transfer using the Kistler force platform.

A multi-body computational study carried out by Meissner [14] was reviewed to further visualize the effects of orientation of the struck limb, in order to adapt real world pedestrian pre-impact motion into the MADYMO pedestrian model [24,30]. Movements of test subjects were captured and kinematic variables of the lower limbs were calculated. Thirty-nine reflective markers were attached onto the volunteers' head, shoulders, trunk, arms, pelvis, legs and feet according to a common biomechanical gait analysis model (Plug-in-Gait, Vicon Nexus) as shown in Figure 7. The human body was divided into fifteen limbs using reflective markers. Walking and running spatial coordinate data was collected. Through this data, the angular position, angular velocity and angular acceleration of the lower limb joints was derived. Time history functions of the joint angles were assigned to the various lower limb joints of the MADYMO pedestrian model to simulate motion.

4. Design of Simulation Matrix

The aim of this study was the application of real life pre-impact variables to simulate real world vehicle-pedestrian accident scenarios. To achieve this, multi-body/FE based complete vehicle/pedestrian system models were developed to simulate real life pedestrian impact events [25].

A parametric simulation matrix was constructed to simulate a comprehensive range of accident scenarios incorporating variables such as vehicle speed, dynamics, pedestrian posture, position and in particular the provision of walking and running gait motion.

For the purpose of this study, the variables defined in Table 1 have been applied to each vehicle model. These pedestrian accident variables were chosen principally for two main reasons: (1) to examine the influence of potential leg fractures, the level of injuries sustained by the pedestrians and kinematics during and after collision; and (2) to qualify the biofidelity definition of the pedestrian lower leg and its ability to effectively simulate the effect of tibia and femur fracture levels. As for the variable range values, these have been derived from the original set of data available in the MADYMO pedestrian human body model [26]. A minimal and maximum variation with regard to the original value was established for the analysis.

A unique naming scheme was applied to each simulation which denotes the vehicle type, vehicle velocity, the pedestrian leg orientation, pedestrian motion type at impact, vehicle braking status and finally the contact position of the pedestrian relative to the vehicle. Each simulation was built manually changing key variables in the MADYMO input deck or keyword file.

Considering the time constraint, decisions had to be made on the selection of the simulation end time and change in configuration of the variables. A Total of 288

individual simulations were performed, out of which simulations using models of the medium and small segment cars were chosen for the trajectory analysis. The results generated from these simulations were used in the calculation of Injury Severity using the IrSiX method.

5. Injury Severity Index (IrSiX) Method

A unique aspect of this study has been the application of the Injury Severity Index (IrSiX) method. The injury results from the simulations were measured and the severity assessed applying a quantitative rating method. This system generates better approximations of severity of injury and consistent repeatability is observed across the range of accident scenarios. In view of the wide range of locations and angles of impact which can be experienced by the head and other parts of the pedestrian's body and recognising the diverse mechanisms by which injury can occur within the body, there is a need for such a rating method. This method of comparative analysis is applied in the laboratory testing of automotive interior structures and components in order to draw comparisons between alternate designs proposed for reducing injury [27, 28].

Injury is a function of both intensity of the loading and the duration of loading. The output measurement of the loading and the duration of loading are integrated together by applying a mathematical weighting factor which best fits the available range of biomechanics data focusing on the injury at the point of impact. An example of this application is the Head Injury Criterion [29]. The large matrix of pedestrian accident simulations which include the influence of varying pre-impact pedestrian kinematics demands an efficient tool to evaluate the outcome of a collision and the computation of global impact injury predictors such as head acceleration and the

forces and moments throughout the body. These variables were built up as matrix from the MADYMO simulations. The assessment of each item of biomechanical data, recorded on the pedestrian during impact is not meaningful as each parameter could have contrary trends. This would make an assessment of the global influence of each parameter rather difficult. Therefore it is necessary to develop a global load index that will contain all load criteria which are representative for the pedestrian biomechanics [27, 28]. This method reflects the importance of the injury criteria and the prediction of the quality of the simulation for different body areas and for a wide range of scenarios in the simulation matrix.

The IrSix formulation is given by:

$$IrSiX = \sum_i (IrSiX)_i = \sum_i (weighting)_i \bullet \frac{(Load\,Value)_i}{(Load\,Limit)_i} \bullet 1000$$

$$\text{With } \sum_i (weighting)_i = 1$$

In order to analyze the extent of injury severity throughout the pedestrian model, biomechanical data for critical body regions of the model were recorded and assessed by applying the weighting factor and the corresponding maximum allowable limit of tolerable injury thus calculating the injury severity index. The principal advantage of the Severity Index is that it eliminates the differences in judgement which are bound to arise even between experienced investigators, and thus permits repeatable and comparable test results to be obtained for a design matrix of simulations.

The IrSiX method provides performance solutions of a simulation matrix, utilizing performance measurement environments where each criterion is able to succeed or fail. This involves aggregating results from multiple runs of the same

underlying model, or in the matrix in which the simulation iterations have been distributed. The sum of all weighting factors is 1 and the total load index (IrSiX) will be 1000 if all the individual load values reach their limit. A Simulation model was constructed using a mid-size FE vehicle model colliding with a stationary pedestrian with an impact velocity of 32km/h (bumper center contact). The resulting performance load index was 888.27, (Table 2) which is less than the total load index (1000). Therefore the results of the simulation were well within the safe performance boundary. This simulation was adapted as a baseline model to which results of all other impact cases from the simulation matrix were compared with.

The results for the mid-size vehicle-pedestrian impact simulation matrix and relevant IrSiX performance levels are as shown in Table 3. Each simulation in the matrix was modelled with varying parameters such as impact speed, pedestrian leg orientation (RLF and LLF) and forward kinematics (Stationary, walking and running pedestrian) and the results were compared to the baseline model results. Statistical models were used to investigate the effects of:

- Pedestrian pre-impact velocity on the outcome of injury severity.
- Vehicle speed and braking.
- Pedestrian position and orientation with respect to the vehicle.

The results identify key characteristics of the impact scenario that cause injury severity in a vehicle pedestrian collision environment. The output results of each of the individual simulations (mid-size car) were analyzed and compared for injury measure such as HIC (head acceleration), Nij (neck injury criteria), chest deflection, pelvis acceleration and fracture of femur, knee and tibia. The results were converted into the IrSiX (global injury index), Table 3.

All simulation models shown in Table 3 are lateral impact cases at center line of the vehicle, no changes were made to the geometry or the stiffness characteristics of the vehicle. From the results it can be seen that the simulations are sensitive to impact speed for almost all injury-related parameters. The parameter study shows a moderate effect of lower leg orientation (gait characteristics) on the severity of the injuries sustained. From observation of simulation 20 (Table 3), due to a contact of the head with the A-pillar, the pedestrian sustains serious injury generating an IrSiX value of 10659.

6. Statistical Analysis of IrSiX Results

In order to further analyze the IrSiX results of 24 simulations (Table 3), responses were categorized by the sensitivity of the simulation models into impact speeds of 32km/h and 40km/h. The responses of variable parameters at two selected velocity levels can also be analyzed by response curves (Logarithmic trend curve) derived by statistical methods (regression techniques). These curves or trend lines indicate the nature and effect (best fit) of individual input variables.

The scatter plots for head, neck, chest, pelvis, femur, knee and tibia were derived from the IrSiX analysis results showing the injury severity. From these curves one can evaluate the effect of pedestrian motion prior to vehicle contact and the influence of pedestrian leg position. Three primary cases were investigated:

- Influence of pedestrian lateral motion with respect to vehicle impact speed.
- Influence of pedestrian leg orientation with respect to vehicle impact speed.
- Influence of vehicle braking with respect to pedestrian lateral motion.

The review of the injury severity trends versus the variables (vehicle velocity, pedestrian lateral motion) is illustrated in Figure 8. Injury severity is strongly dependant on the vehicle velocity. 40km/h trend curve shows a higher HIC, as in most

cases higher impact speed results in higher injury severity. The trends also show a high degree of sensitivity towards pedestrian lateral motion. The HIC reduces as the pedestrian is simulated with motion.

Figure 9 shows the effect of leg position, either left leg forward (LLF) or right leg forward (RLF) prior to impact. From the trends it is evident that the initial pedestrian stance and leg orientation has a significant effect on the HIC, as in the case of RLF contact in both impact speeds of 32 and 40km/h, the injury severity is higher particularly when the pedestrian is standing still but decreases as the pedestrian is simulated with gait motion. In contrast, there is an increase in HIC as the pedestrian is simulated with gait motion (from static to running gait) in LLF contact cases.

Of interest in this section, is the influence of vehicle braking on the pedestrian injury severity. The results in Figure 10 show the influence of vehicle braking on pedestrian HIC. The results also show effects of variables such as pedestrian lateral motion and pedestrian leg orientations. Emergency braking with a deceleration of 0.75 g is applied during the impact event and the braking is applied just before contact with the pedestrian.

Each trend line shows the relative effect of vehicle deceleration or the lack of it prior to impact. Different trend line markers have been assigned to show the influence of leg orientation which is either the left (LLF) or right leg (RLF) forward contact. The RLF contact type for both vehicle braking and non-braking scenario generates higher severity compared to the LLF in the static case. In cases of walking and running impacts, injury severity is higher in LLF impacts when compared to RLF impacts. This increase in injury severity in LLF (non-struck leg) impact simulations is due to the fact that the upper body of the pedestrian rotates clockwise about its vertical axis.

The results from these simulations have been used to investigate the effect of pedestrian gait motion and leg orientation. Injury severity as a result of pedestrian lateral motion (walking and running) was found to be comparatively higher than for a static pedestrian. It is observed that the tibia and the knee influence high injury in static pedestrian cases due to the direct contact with the bumper. The femur and the pelvis influence high injury in walking pedestrians due to contact with the bumper and bonnet leading edge. In the case of the running pedestrians, the femur, pelvis, thorax and the head influence high trauma due to the combination of increased velocity and gait phase at point of impact.

7. Analysis of Pedestrian Trajectory

Lateral motion of pedestrians, has an influence on post impact trajectory. During walking and running, the body's center of mass, oscillates vertically and horizontally, as it moves over the supporting leg, until the opposite leg is brought forward. The inertia of the body increases and decreases during walking and running gait cycle but is highest during running. This results in pedestrian's upper body moving forward even after the lower extremities come into contact with the front end of the vehicle. Post impact trajectory is sensitive to factors such as pedestrian height, lateral pedestrian velocity and contact characteristics between pedestrian and vehicle.

Vehicle-pedestrian accident simulations having walking and running motion were compared to static pedestrian collisions and pedestrian projection distance in each scenario was measured. It can be seen in Figure 11 that the distance travelled after impact by the running pedestrian is slightly higher than in the other two cases.

This study investigates further in detail, the potential effect of leg orientation on post impact trajectory. Pedestrians were modelled with left leg forward and right leg forward during impact as can be seen in Case study 1 and 2.

Case 1: Small Segment car-32km/h Impact with Left-Leg Forward Pedestrian

Figure 12 shows the general trajectory taken by the pedestrian's pelvis until the pedestrian comes into contact with the ground. The impact velocity of the small segment car is 32km/h. Figure 12 also shows the post-crash motion of walking and running pedestrian in comparison to static pedestrian. In this scenario, the pedestrian had his left leg forward during impact.

Observation of Figure 12, suggests that there exists a substantial shift in the trajectory in the direction of lateral motion with maximum deviation in the case of the running pedestrian simulation. There exists minor difference in forward projection between the simulations. When left leg forward simulations are observed closely, the difference in the position of head contact on the windscreen changes as the pedestrian is simulated with walking and running motion. The upper body of the pedestrian keeps moving further even after the lower extremities have made contact with the bumper and bonnet edge.

Case 2: Small Segment car-32km/h Impact-Right Leg Forward Pedestrian

Similar effect of leg orientation on pedestrian post impact trajectory exists in right leg forward pedestrian impact cases (Figure 13). The major difference between the right leg forward and the left leg forward impacts is the direction of rotation of the pedestrian through his vertical axis which can be seen as clockwise rotation for left

leg forward pedestrians and anti-clockwise rotation for right leg forward impacts. This rotation causes the pedestrian's forehead/temple area to contact the windscreen in the case of left leg forward impact scenarios and the area of the occiput contacts the windscreen in later case.

This change in trajectory is in the direction of motion. In general, trajectory of the head tends towards the a-pillar as the pedestrian is simulated with increased lateral motion (walking/ running). This increases the probability of injury as the head moves closer to the rigid part of the windscreen.

The motion of the pedestrian increases the wrap distance and hence the head to windscreen contact time increases. Figure 14 shows the head impact time in both right and left leg impact scenarios for a small segment vehicle.

Figure 14 shows the head impact time in right leg impact scenarios for a small segment vehicle. The trajectory of the head tends towards the a-pillar in moving pedestrian impact cases. The rotation of the pedestrian through his vertical axis is evident (clockwise rotation and anti-clockwise rotation of pedestrian). A similar effect of leg orientation is also seen in medium segment car-pedestrian impacts. The head to windscreen contact time decreases as the impact velocity of the vehicle increases from 32km/h to 40km/h.

8. Conclusions

The walking and running simulations have provided significant improvements over the standing pedestrian model. Taking into account the forward walking or running motion, the impact simulations have generated true multi-planar life like responses. Injury severity as a result of pedestrian lateral motion was found to be comparatively higher than for a static pedestrian. This reinforces the findings that the real world

simulations with pedestrian motion are likely to cause more injury than the static pedestrian simulations. Both the computer simulation techniques and the pedestrian simulation database have provided results which will allow future analysis and development to take place. The Injury Severity Index (IrSiX) approach and methodology will contribute to the development of injury prediction tools in the automotive industry.

This research encompasses a wide range of real-world vehicle-pedestrian accident scenarios and has been assessed using MADYMO. The application of different research methods such as mathematical modelling, crash analysis and testing, provide the most effective approach to understand, solve and gain confidence in vehicle-pedestrian accident simulations.

Table 1. Simulation Variables Selected for this Study

Simulation Variables (V)	Variables Range		
V1 Vehicle velocity	32km/h	40km/h	
V2 Pedestrian velocity	0Km/h	7Km/h	11Km/h
V3 Pedestrian lateral position	86cm left from center	Center(zero)	86cm right from center
V4 Pedestrian posture	left leg forward	right leg forward	
V5 Vehicle braking	no braking	with braking	

Table 2. Σ IrSiX results for baseline simulation

IrSiX	Head	Neck up	Thorax	Pelvis	Femur	Knee	Tibia	Σ IrSiX
Σ comp IrSiX	200	190	200	100	190	100	20	1000
Baseline simulation	250.2	155.6	177.7	141.2	73.1	61.5	28.92	888.27

Table 3. IrSiX Results for mid-sized car-pedestrian impacts at center line of vehicle.

				IrSiX Comp	Head	Neck up	Thorax	Pelvis	Femur	Knee	Tibia	Σ IrSiX
				Σ IrSiX Threshold	200	190	200	100	190	100	20	1000
Simulation	Speed (km/h)	Braking	Posture	Leg Orientation								
1	32	Off	Static	Right Leg Forward	592.9	266.8	326.6	201.5	108.6	62.5	29.54	1588.5
2	32	Off	Static	Left Leg Forward	236.9	126.2	43.3	37.6	43.1	73.5	35.85	596.4
3	32	On	Static	RLF	250.2	155.6	177.7	141.2	73.1	61.5	28.92	888.3
4	32	On	Static	LLF	215.6	104.3	34.1	34.1	45.1	70	35.69	538.9
5	40	Off	Static	RLF	525	184.9	220.3	250.1	219.2	68.3	29.38	1497.1
6	40	Off	Static	LLF	339.2	134	61.1	35.2	67.3	62.5	35.85	735.1
7	40	On	Static	RLF	427.5	174.4	84.1	282.9	251	64.3	29.77	1314.0
8	40	On	Static	LLF	302.7	113.3	42.2	37.7	89.3	79.5	37.62	702.3
9	32	Off	Walking	RLF	218.5	102.3	650.6	189.2	153.6	64	24.77	1403.0
10	32	Off	Walking	LLF	307	210.4	283.8	36.8	52.9	64	32.54	987.4
11	32	On	Walking	RLF	194.4	206.8	213.8	155.8	158.5	60	23.77	1012.9
12	32	On	Walking	LLF	243.2	109.3	77.3	29.8	47.3	65.5	32.31	604.7
13	40	Off	Walking	RLF	313.5	142.1	98.9	295.4	225.1	73	29.23	1177.3
14	40	Off	Walking	LLF	444.2	279.2	517.9	93.9	67	78.5	35.92	1516.6
15	40	On	Walking	RLF	257.9	132.8	80.3	245	212.5	67	28.62	1024.2
16	40	On	Walking	LLF	400.3	211.5	208.2	87.4	173.5	75.5	35.31	1191.8
17	32	Off	Running	RLF	157	97.2	52.3	114.9	120.2	47	23.46	612.1
18	32	Off	Running	LLF	282.2	143.3	483	33.3	61	61.3	32.31	1096.3
19	32	On	Running	RLF	126.7	94.7	69.9	89	134.8	49.5	25.08	589.7
20	32	On	Running	LLF	10659.3	341.4	91.2	27.2	60.4	63	31.08	11273.5
21	40	Off	Running	RLF	367.1	153.2	88.1	158.2	361	59.5	29.38	1216.5
22	40	Off	Running	LLF	475	263	626.4	315	263.9	68.8	30.62	2042.6
23	40	On	Running	RLF	336.5	147.8	82.1	152	394.2	58.8	28.85	1200.2
24	40	On	Running	LLF	447.7	277	574.4	45.5	70	68.5	32.69	1515.9

Figure 1. FE/FACET Vehicle Models

Figure 2. Test setup of FE/FACET Vehicle Model and MB Pedestrian Model

Figure 3. Trajectory comparison of Pedestrian impacted by a mid-size vehicle at 32km/h

Figure 4. Resultant Head Velocity

Figure 5. Pedestrian Head Acceleration

Figure 6. Pedestrian Tibia Acceleration

Figure 7. Gait Analysis of pedestrian motion using VICON system

Figure 8. Effect of Vehicle Velocity and Pedestrian Lateral Motion Type on HIC

Figure 9. Effect of Pedestrian Lateral Motion and Leg Position Type on HIC

Figure 10. Effect of Vehicle Braking and Lateral Motion Type on HIC

Figure 11. Trajectory comparison with static, walking and running impact scenarios

Figure 12. 32km/h impact with left leg forward moving pedestrian

Figure 13. 32km/h Impact with Right Leg Forward Pedestrian

Figure 14. Head Trajectory in left-leg and right-leg forward 32km/h impacts

References

[1]. DVLA and Department for Transport (DfT)(2009). Transport trends: 2009 edition.

[2]. Department for Transport (DfT)(2007). Road Accident Statistics Fact sheet-3 (Nov 2008).

[3]. EEVC/CEVE WG17 Report, (1998). Improved test methods to evaluate pedestrian protection afforded by passenger cars. Working Group 17 Report.

[4]. MADYMO (1997). MADYMO Version 5.4 Manuals. TNO Road-Vehicle Institute, Delft, Netherlands.

[5]. Kühnel, A., Appel, H., Stürtz, G., and Glöckner, H., (1978). Pedestrian safety Vehicle-Design Elements-Results of in-depth accident analyses and simulation, Proc. 22nd Annual AAAM, pp. 132-153.

[6]. Happer, A., Araszewski, M., Toor, A., (2000). Comprehensive analysis method for vehicle/pedestrian collisions. SAE Pp 2000- 01-0846.

[7]. Pasanen, E., (1993). The video recording of traffic accidents. Helsinki City Planning Publications.

[8]. Eubanks, J., Hill, P., (1998). Pedestrian Accident Reconstruction. Lawyers and Judges publishing. Co., Tuscon, AZ.

[9]. Eubanks, J., Haight, W.R., (1992). Pedestrian Involved Traffic Collision Reconstruction Methodology. SAE Paper 921591.

[10]. Breniere, Y., Do, M., (1986). When and how does steady state gait movement induced from upright posture begin? Journal of Biomechanics, Volume 19, No. 12, pp 1035-1040.

[11]. Fugger, T., Randles, J., Eubanks, J., (2002). Pedestrian throw kinematics in forward projection collisions. SAE Pp. 2002-01-0019.

[12]. Stammen, J.A., (2002). A Demographic analysis and reconstruction of selected cases from the pedestrian crash data study. SAE Pp 2002-01-0560.

[13]. Le Glatin, N., Blundell, M., Blount, G., (2003). The simulation of pedestrian impact with a combined multibody finite elements system model. Journal of Engineering Design, Vol. 17, No. 5. (October 2006), pp. 463-477.

[14]. Meissner, M., Rooij, L., Van., Bhalla, K., Crandall, J., Longhitano, D., Takahashi, Y., Dokko, Y., Kikuchi, Y., (2004). A Multi – Body Computational Study of the Kinematic and Injury Response of a Pedestrian with variable stance upon impact with a vehicle. SAE 2004 World Congress, SAE pp 2004-01-1607.

[15]. RCGB (2007). Transport Statistics Bulletin Annual Report.

[16]. Le Glatin, N., Blundell, M., Blount, G., (2003). An analysis methodology for the simulation of vehicle pedestrian accidents. Proc. IMechE Conference on Statistics and Analytical Methods in Automotive Engineering, Professional Engineering Publishing, ISBN 1 86058 387 3, pp. 197-206.

[17]. Konosu, A., Ishikawa, H., Kant, R., (2000) "Development of computer simulation models for pedestrian subsystem impact tests", JSAE 21 (2000) 109-115.
[18]. Kant, A.R., (1997). EEVC WG-10 legform impactors MADYMO database development, July 1997.
[19]. Ishikawa, H., Kajzer, J., (1993). Computer Simulation of Impact Response of the Human Body in Car-Pedestrian Accidents. Proc. of the 37th STAPP Car Crash Conf. Nov 8-10, San Antonio, Texas. Pp 135-248.
[20]. Ishikawa, H., Kajzer, J., Ono, K., Sakurai, M., (1994). Simulation of car impact to pedestrian lower extremity: influence of different car-front shapes and dummy parameters on test results. Accid Anal Prev 1994, 26:231-42.
[21]. Ishikawa, H., Konosu, A., Akiyama, A., Yoshida S., Matsuhashi T., Moss S., and Salloum, M., (1999). Development of Human-like Pedestrian Dummy, Paper 9934546, Japanese Society of Automotive Engineers, Chiyoda-Ku, Tokyo, Japan.
[22]. Masson, C., Serre, T., Cesari, D., (2007). Pedestrian-vehicle Accident: Analysis of 4 Full Scale Tests with PMHS. Experimental Safety Vehicles Conference, Lyon, France. Scientific Direction. French National Institute for Transport and Safety Research, Paper 07-0428.
[23]. Horward, M., Thomas, A., Koch, W., (1999). Validation and Application of Finite Element Humanoid Model for use in Pedestrian Accident Simulation. Ford Forschunszentrum Aachen GmbH.
[24]. Simms, C.K., Woods, D.P., (2006). Effects of Pre-impact Pedestrian Position and Motion on Kinematics and Injuries from Vehicle and Ground Contact. International Journal of Crashworthiness, Volume 11, Pages 345-355.
[25]. Untaroiu, C.D., Shin, J., Ivarsson, J., Crandall, J.R., Subit, D., Takahashi, Y., Akiyama, A., Kikuchi, Y., (2008). A Study of the Pedestrian Impact Kinematics using Finite Element Dummy Models: the Corridors and Dimesional Analysis Scaling of Upper-Body Trajectories. Int. Journal of Crashworthiness Volume 13 pp 469-478.
[26]. De Lange, R., Happee, R., (2000). MADYMO Pedestrian Models Manual. TNO Road Vehicles Institute, Delft, Netherlands.
[27]. Uhl, Edgar (11th Dec 2006). The use of the IrSiX – Factor. HeliSafe TA. Co-ordination memorandum AFG- 32-00017.
[28]. HeliSafe- Helicopter Occupant Safety Technology Application, (2004-2007). A European research project in the sixth framework programme of the European commission. Autoflug GmbH Industriestrasse 10, D-25462 Rellingen.
[29]. Prasad, P., and Mertz, H., (1985). The position of the U.S Delegation to the ISO Working Group 6 on the use of HIC in the automotive environment. SAE paper 851246.
[30]. Soni, A., Chawla, A., Mukherjee, S., Malhotra, R., (2010). Effect of muscle contraction on the lower limb response in low speed car–pedestrian lateral impact: simulations for a walking pedestrian, International Journal of Crashworthiness, 1754-2111, Volume 15, Issue 5, 2010, Pages 543 – 551.
[31]. Untaroiu, C.D., Shin, J., Ivarsson, J., Crandall, J.R., Subit, D., Takahashi, Y., Akiyama, A., Kikuchi, Y., (2008). A study of the pedestrian impact kinematics using finite element dummy models: the corridors and dimensional analysis scaling of upper-body trajectories International Journal of Crashworthiness, 1754-2111, Volume 13, Issue 5, 2008, Pages 469 – 478.

[32]. Untaroiu, C.D., Shin, J., Crandall, J.R., (2007). A design optimization approach of vehicle hood for pedestrian protection. International Journal of Crashworthiness, 1754-2111, Volume 12, Issue 6, 2007, Pages 581 – 589.
[33]. Matsui, Y., Ishikawa, H., Sasaki, A., (2006). Proposal of injury risk curves for evaluating pedestrian femur/pelvis injury risk using EEVC upper legform impactor based on accident reconstruction. International Journal of Crashworthiness, 1754-2111, Volume 11, Issue 2, 2006, Pages 97 – 104.
[34]. Yang, J., (1997). Mathematical simulation of knee responses associated with leg fracture in car-pedestrian accidents. International Journal of Crashworthiness, 1754-2111, Volume 2, Issue 3, 1997, Pages 259 – 272.

Figure
Click here to download high resolution image

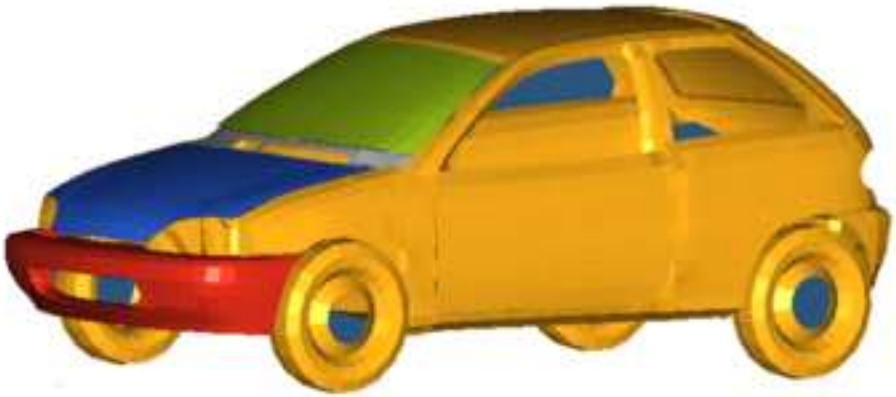

Small segment car

Mid-size car

People carrier

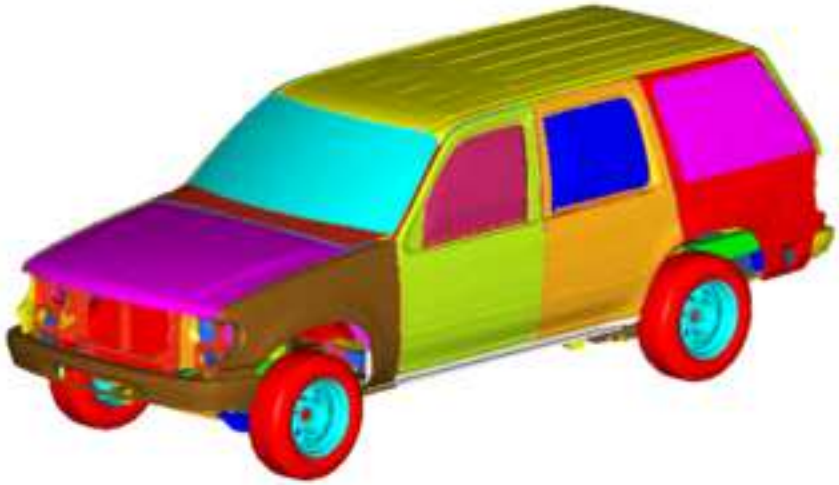

Sports Utility Vehicle

Figure

Click here to download high resolution image

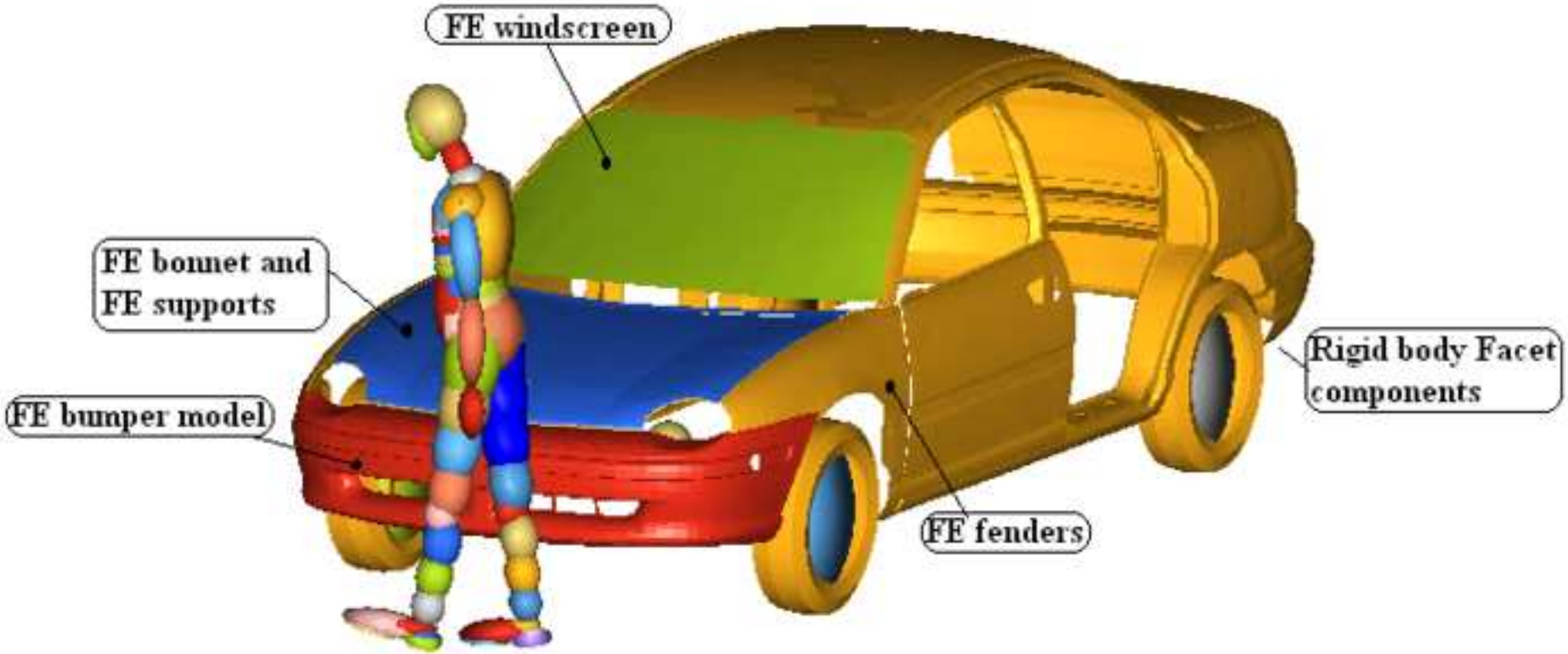

Figure
Click here to download high resolution image

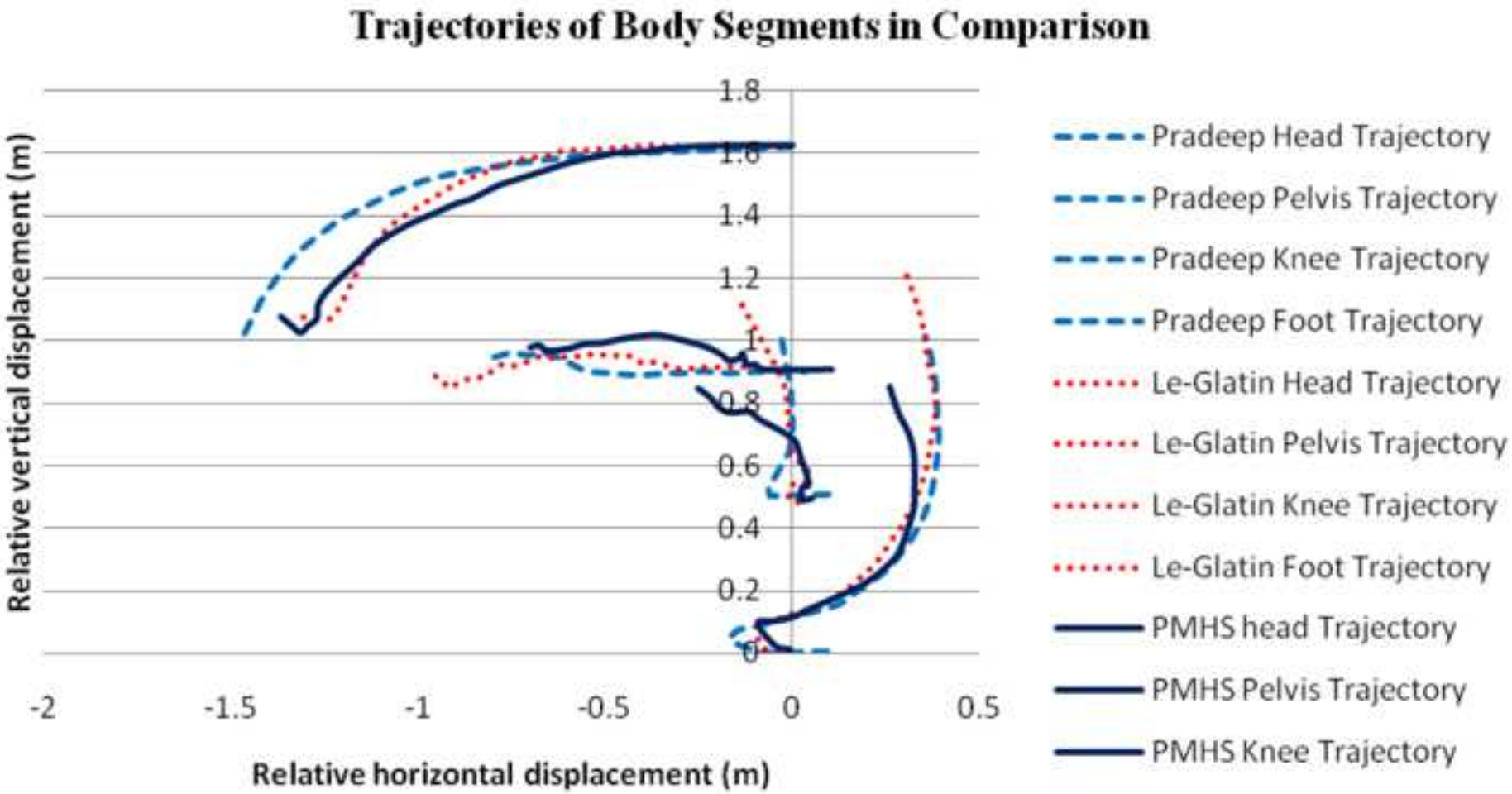

Figure

Click here to download high resolution image

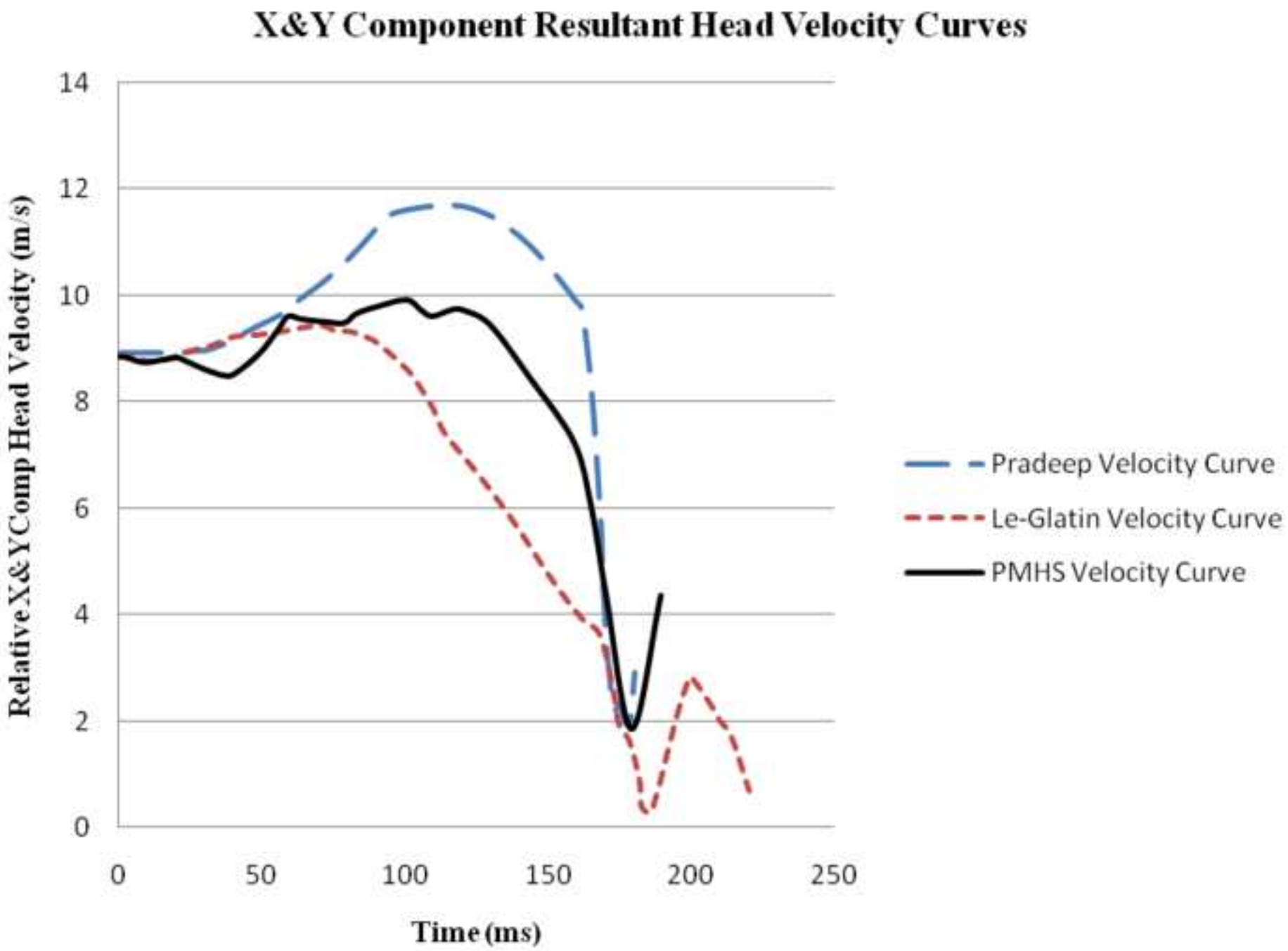

Figure

Click here to download high resolution image

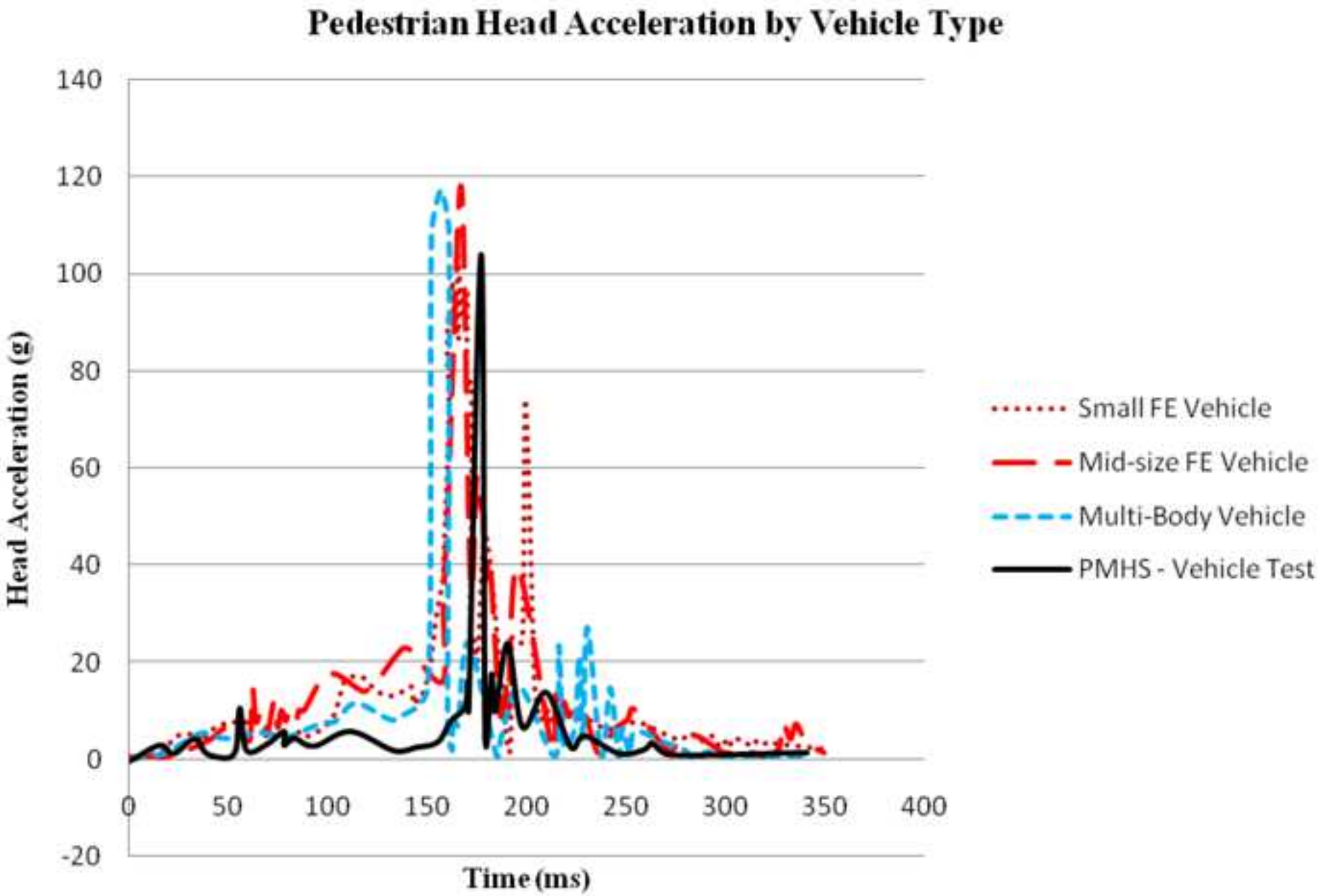

Figure

Click here to download high resolution image

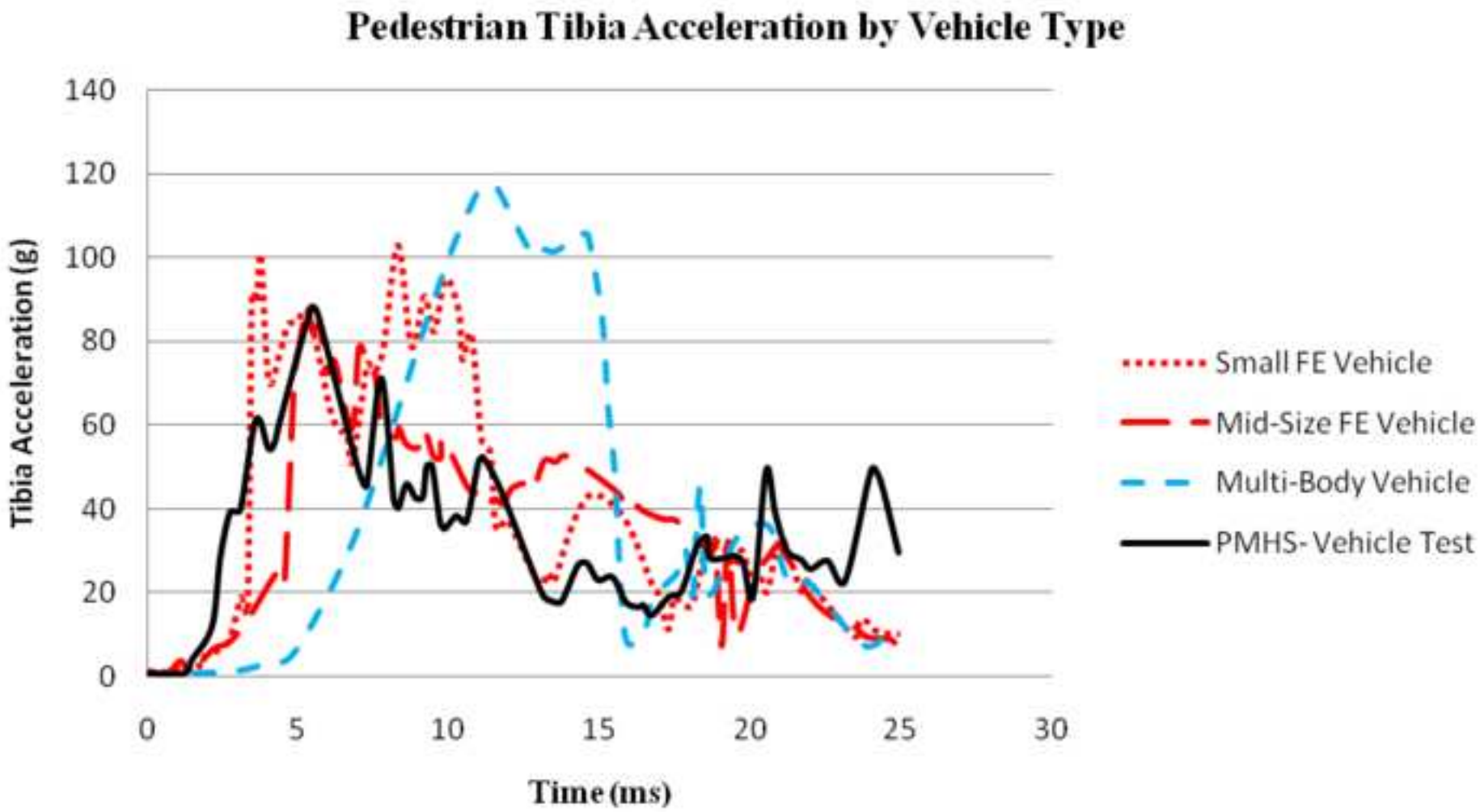

Figure

Click here to download high resolution image

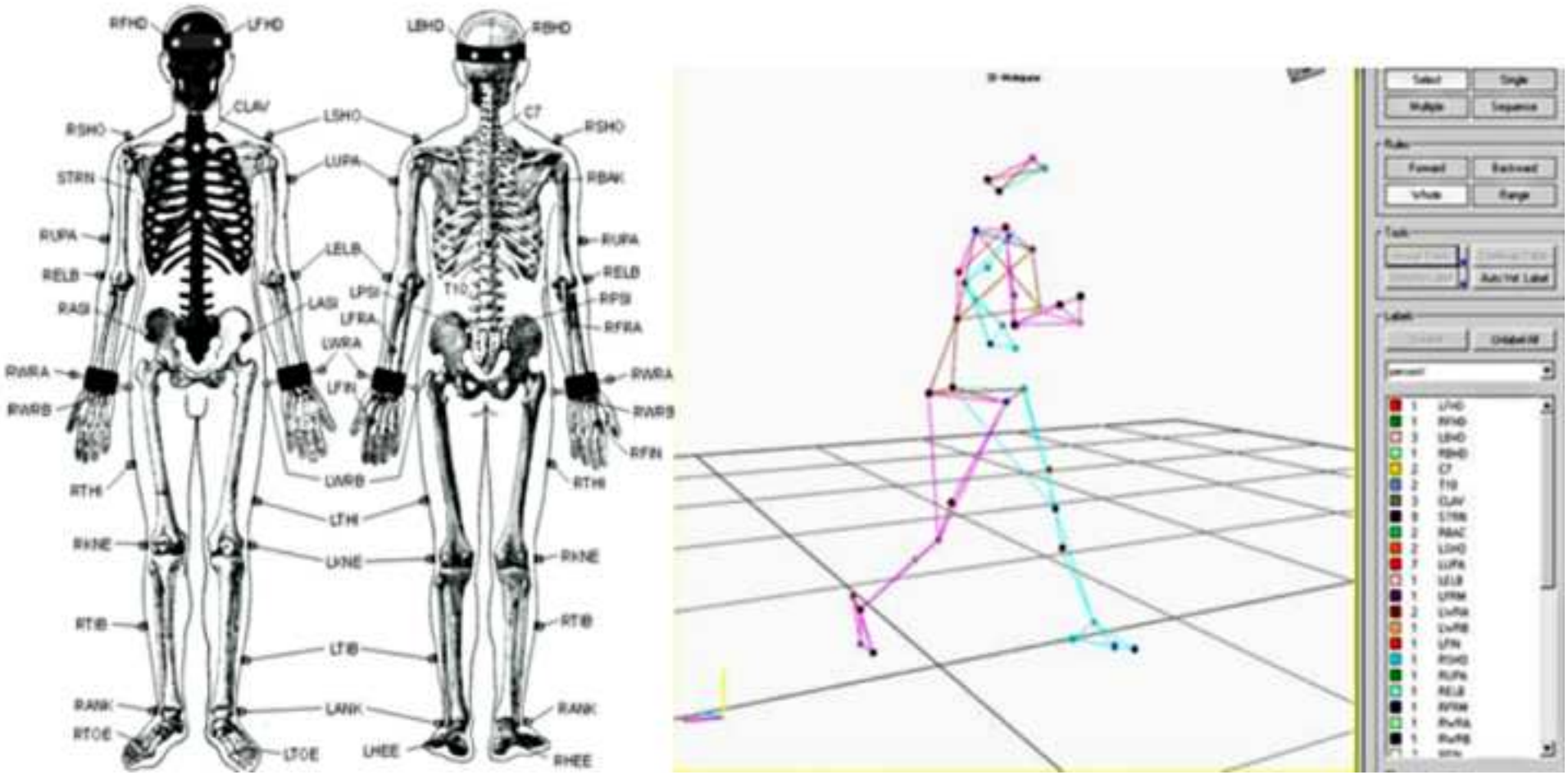

Figure

Click here to download high resolution image

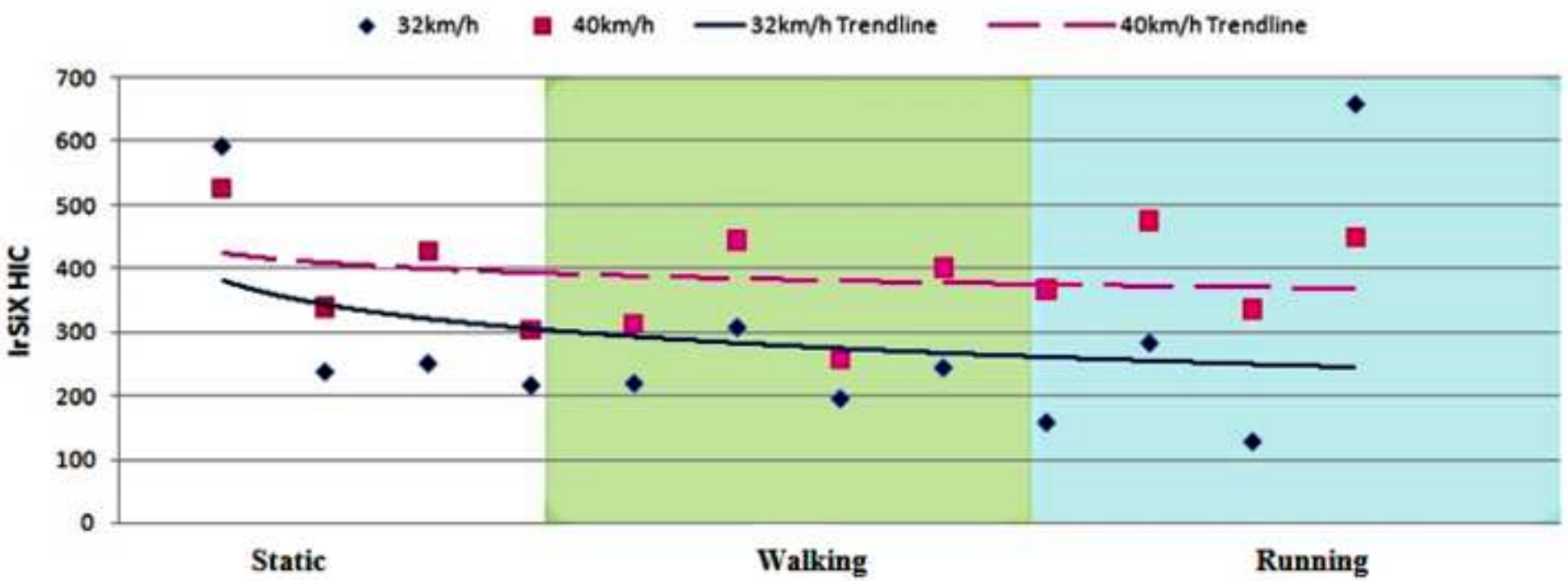

Figure
Click here to download high resolution image

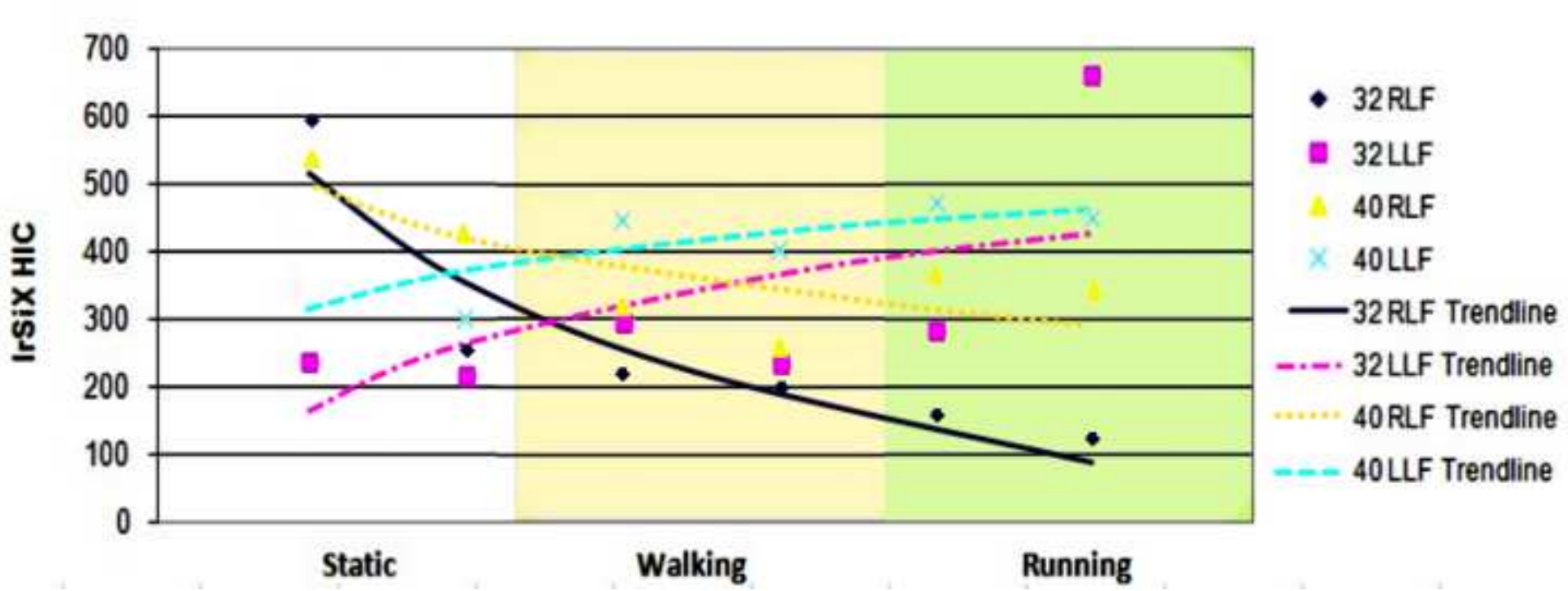

Figure

Click here to download high resolution image

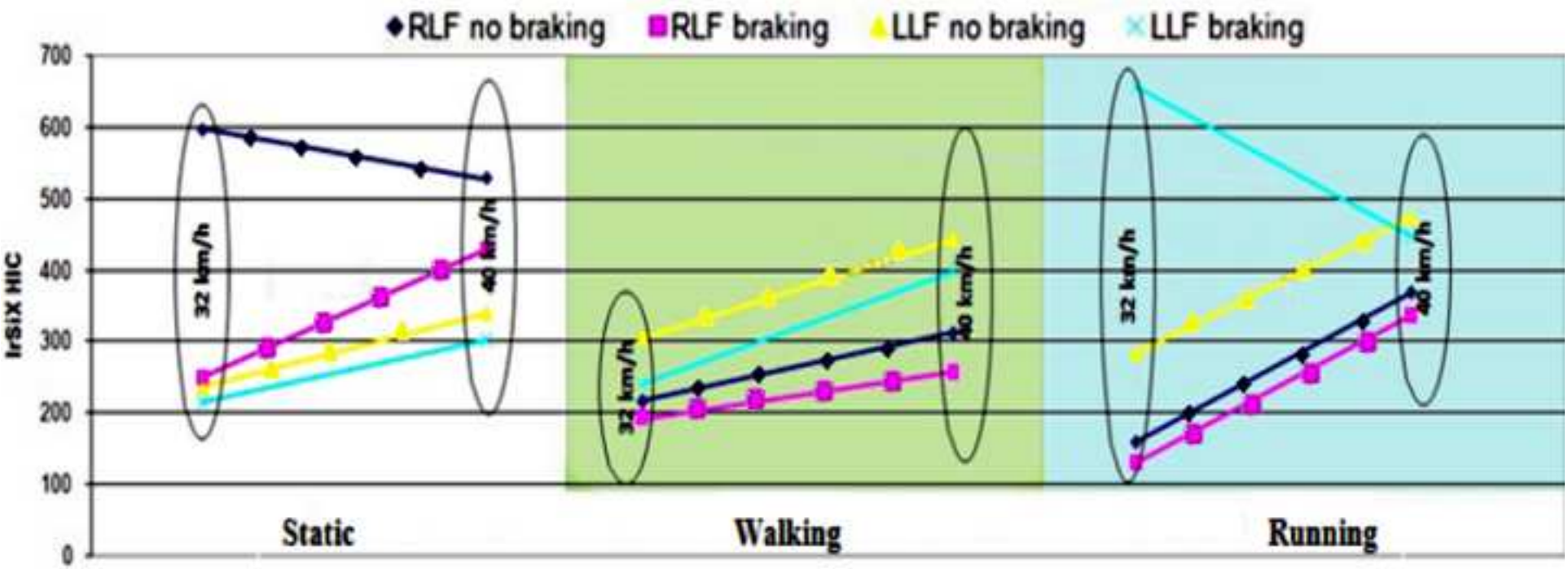

Figure

Click here to download high resolution image

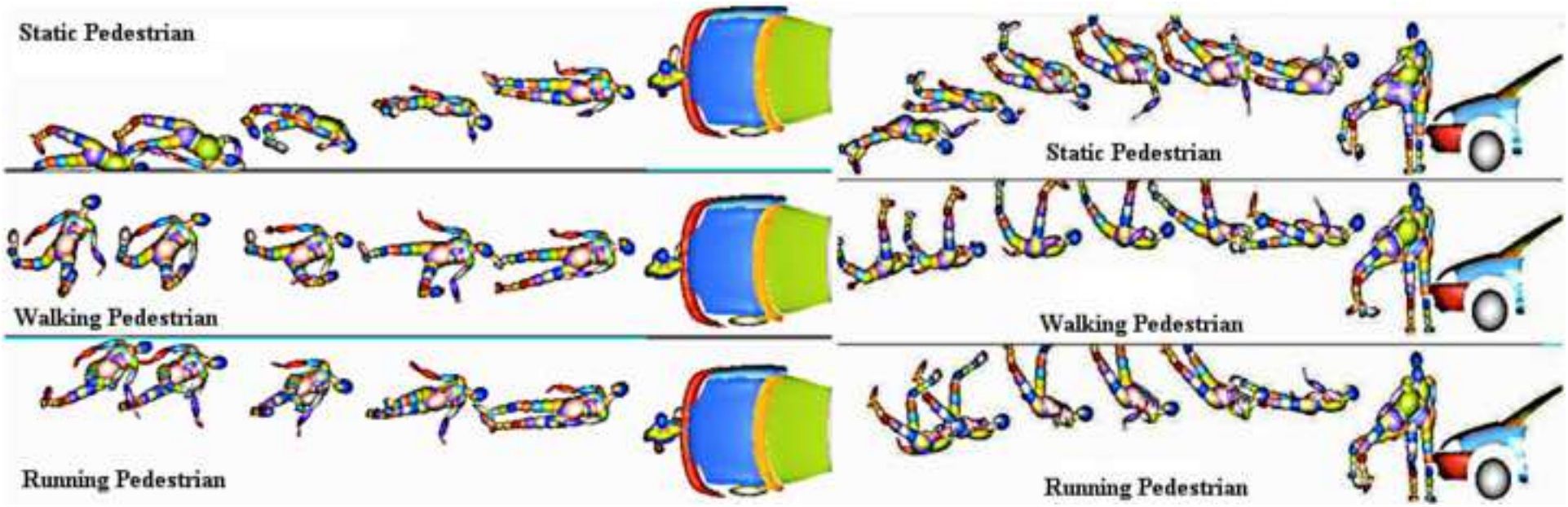

Figure

Click here to download high resolution image

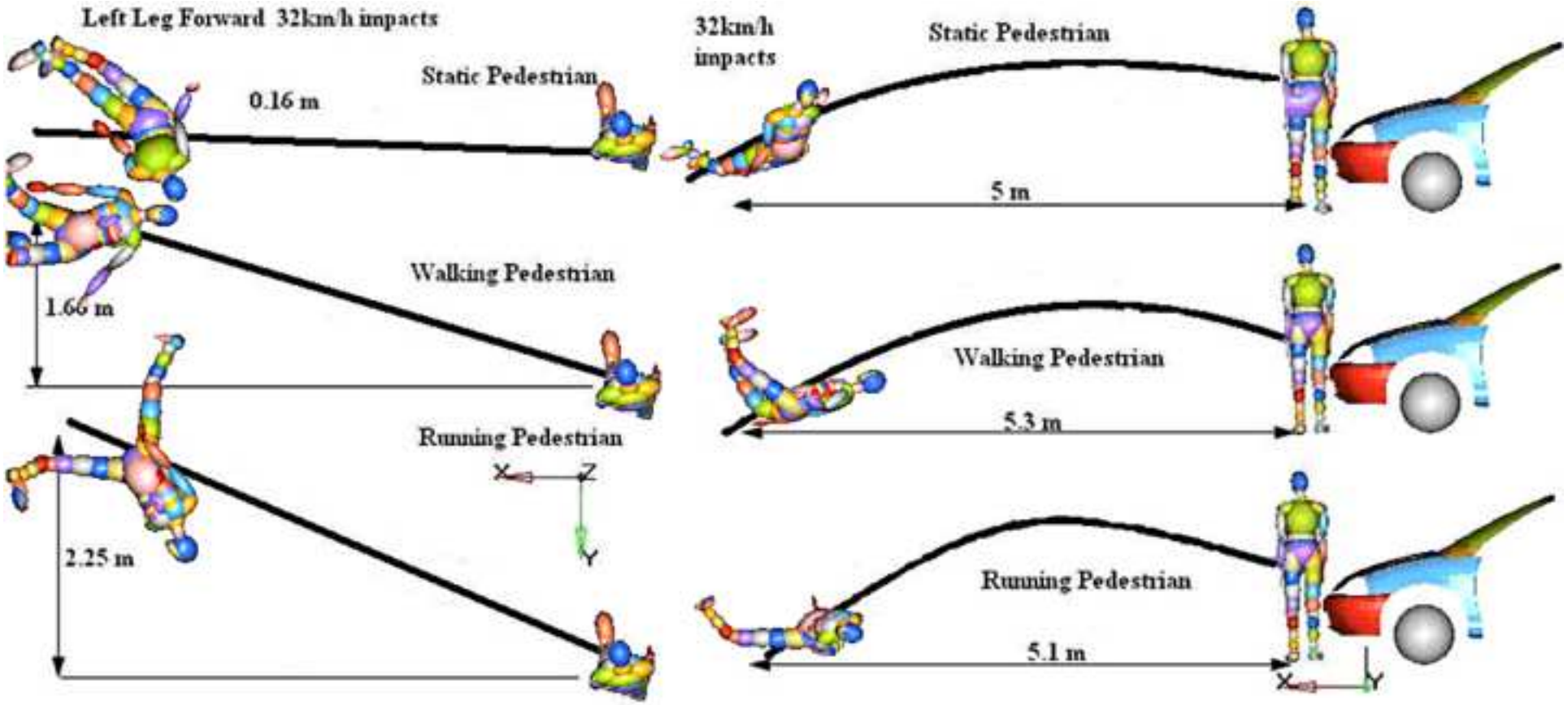

Figure

Click here to download high resolution image

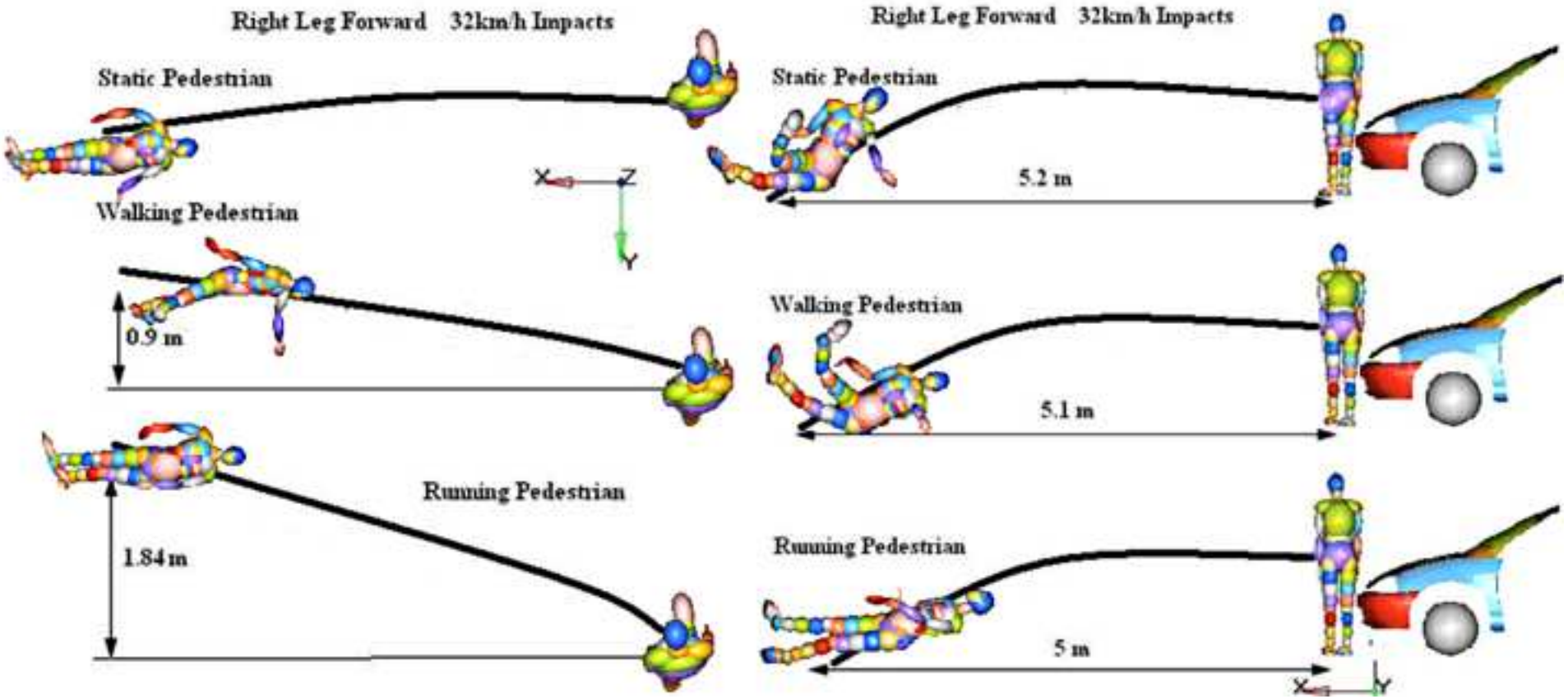

Figure

Click here to download high resolution image